

# ASSESSMENT OF SEEPAGE IN AN EMBANKMENT DAM USING VERY LOW FREQUENCY ELECTROMAGNETIC AND GEOELECTRICAL METHODS

## ABSTRACT

Geophysical surveys involving Very Low Frequency Electromagnetic (VLF-EM), Vertical Electrical Sounding (VES) and 2D resistivity imaging were conducted along the embankment of Asejire dam to detect potential seepage zones and assess the integrity of the dam. 750 VLF-EM measurements were made at 10 m station interval using the VLF-EM Equipment. 24 Schlumberger VES were conducted at 20 m interval using resistivity meter and its accessories. The current electrode spacing ( $AB/2$ ) was varied from 1 m to 100 m. The 2D resistivity profiling employed the dipole-dipole configuration with electrode spacing,  $a = 20$  m and expansion factor,  $n = 1 - 5$ . The VLF-EM data were processed and modelled using Fraser Filtering and Karous-Hjelt software to delineate subsurface zones of varying conductivities suggesting anomalous seepage. The VES data were quantitatively interpreted using the partial curve matching technique and 1D resistivity inversion algorithm while the dipole-dipole data were inverted using 2D resistivity inversion procedure. The VLF-EM inverted sections revealed prominently conductive zones indicating anomalous seepage zones beneath the dam embankment. The relatively less conductive zones possibly indicate reduced seepage. The results of VES interpretation revealed three geoelectric layers beneath the dam embankment representing the caprock, core and bedrock. The 2D inverted resistivity sections delineated zones with anomalously low resistivity generally less than  $10 \Omega\text{m}$ , indicating anomalous seepage, beneath the embankment. This study has demonstrated the effectiveness of combining the VLF and geoelectrical methods for delineating anomalous seepages in the assessment of dam safety. The anomalously low resistivity/high conductive zones identified beneath the dam embankment are suspected anomalous seepage zones which can threaten the integrity of the dam. Routine monitoring and remedial measures are therefore recommended to forestall the failure of the dam.

**Keywords:** Embankment, resistivity low, high conductivity, anomalous seepage, Asejire.

## INTRODUCTION

A dam is a structure built across a river or stream to impound water for irrigation, domestic, industrial, hydropower generation, or recreational use (Camarero and Moreira, 2017, Ahmed *et al.*, 2023). It also helps to control flooding by slowing down water flow during heavy rainfall on the upstream side to prevent over flooding downstream. An embankment dam is typically composed of fragmented independent rock and/or soil materials compacted into a complex, semi-plastic mound whose heavy weight helps to resist the pressure of the water from the reservoir. The friction and interaction of the soil and rock particles bind them together into a stable mass without cementing substance. The surface is covered by waterproof natural materials to make the dam impervious to surface erosion while the core is made of dense, impervious soil such as clay to prevent seepage through the structure.

Dams are designed to allow very low amount of seepage through it beyond which seepage becomes a problem as it threatens the structural integrity of the dam (Mugawata *et al.*, 2020b). Anomalous seepage is prominent among the major causes of dam failure which also include internal erosion, foundation failure, overtopping, static and seismic instability (Boneli, 2013, Lyu *et al.*, 2019).

The existence of faults, fractures, joints, fissures or shear zones in bedrock and discontinuities in the embankment provides pathways for seepage which may reduce impoundment of water in the reservoir area if it becomes intolerable. Anomalous seepage constitutes serious threat to structural integrity of dams and may lead to dam failure and loss of lives and property on the downstream side if it is not redeemed (Okpoli and Tijani, 2016).

It is therefore important to carry out post-construction checks and monitoring of dam regularly in order to detect possible breach or damage in the dam structure. Routine monitoring of seepage involves investigation of dams for changes within and beneath the embankment and is useful to detect seepage problem early and propose to execute remedial measures to avert structural failure (Ahmed *et al.*, 2023). Most dam failure occurred because seepages through the dams were not checked and monitored after construction.

Geophysical methods are generally employed in damsite feasibility studies involving foundation investigation, geological and structural mapping of both embankment and reservoir floor. The methods are non-invasive, faster and cheaper than other direct investigative methods (Sharma, *et*

*al.*, 2014, Sungkono *et al.*, 2014, Adamo *et al.*, 2020, Golebiowski *et al.*, 2021). They are also applied during and after the construction phase to delineate subsurface geological sequences, and reveal lithological variation(s) which may threaten structural integrity in the dam.

Very Low Frequency Electromagnetic (VLF-EM) and Electrical Resistivity methods are the two principal geophysical methods usually employed in dam embankment investigation since they are rapid and cost effective. The VLF-EM and 2D resistivity imaging methods can detect anomalous seepages as high conductivity and resistivity low anomalies respectively. Both methods are capable of detecting internal erosion processes and anomalous seepage within a dam embankment at an early stage before the safety of the dam is at stake (Okpoli and Tijani, 2016, Camarero and Moreira, 2017, Akinlabi and Ayanrinde, 2018, Olasunkanmi *et al.*, 2021, Hung *et al.*, 2020, Mugawata *et al.*, 2020a).

Based on the afore-mentioned, Very Low Frequency Electromagnetic (VLF-EM) and Electrical Resistivity surveys involving Schlumberger vertical electrical sounding (VES) and 2D resistivity imaging using the dipole-dipole array were carried out along the embankment of Asejire dam, Ibadan, southwestern Nigeria, to assess the level of seepage and integrity of the dam in. The objectives are to determine the geoelectric parameters of the subsurface layers, determine the lateral and vertical resistivity/conductivity variations in the subsurface strata, delineate the subsurface lithological units, and map possible seepage zones within the embankment.

### **Study area**

The study area is located in Asejire town about 30 km east of Ibadan. It lies within latitude  $7^{\circ} 21.5' N - 7^{\circ} 22' N$  and longitude  $4^{\circ} 07.68' E - 4^{\circ} 08.26' E$  (Fig. 1). Asejire embankment dam is a combination of earth-fill and rock-fill dam separated by a spill-way which provides controlled passage for surplus water downstream when the reservoir is full. to prevent overtopping. It was built in the late 1960s to impound water from River Osun and provide water for the Asejire and Osegere water treatment plants to supply domestic and industrial water for Ibadan and its environs (Asibor, 2015). The dam embankment is about 818 m long while the dam crest elevation of about 159.4 m. The dam has a capacity of about 8 million litres per day, 80% of which is used for domestic purposes (Oladimeji and Olaosebikan, 2017, Utete and Fregene, 2020). The area is covered by an admixture of savanna and high forest trees with palm,

characteristic of secondary rainforest vegetation (Ajani *et al.*, 2014). It has numerous low hills with very gentle slopes and is mainly accessible by Ibadan-Ife expressway, secondary road and foot paths.

The study area is underlain by Precambrian crystalline basement rocks of southwestern Nigeria typically migmatite gneiss (Fig. 2) exposed as low lying outcrops on the downstream side. Migmatite gneiss is a high-grade foliated, fine-to-medium grained metamorphic rock characterized by distinct banding of alternating light (felsic/potassic) and dark (mafic) minerals reflecting partial melting (Ajigo *et al.*, 2019, Balogun *et al.*, 2019, Ademila, 2022). The main constituent minerals are quartz, feldspar, plagioclase, hornblende biotite and muscovite (Pawley *et al.*, 2015, Akinola and Obasi, 2020).

## **METHODOLOGY**

### **Electromagnetic Profiling**

The VLF-EM and resistivity surveys were carried out along both flanks of the dam embankment (Fig. 3). 750 VLF-EM measurements were made at station interval of 10 m with the WADI VLF-EM Equipment. Both filtered real and filtered imaginary were recorded. The VLF-EM data were processed using the Fraser filtering technique, to improve the signal-to-noise ratio and improve the resolution of the anomalies (Fraser, 1989). They were then subjected to 2D inversion using Karous-Hjelt software which inverted the ratios of the secondary to primary

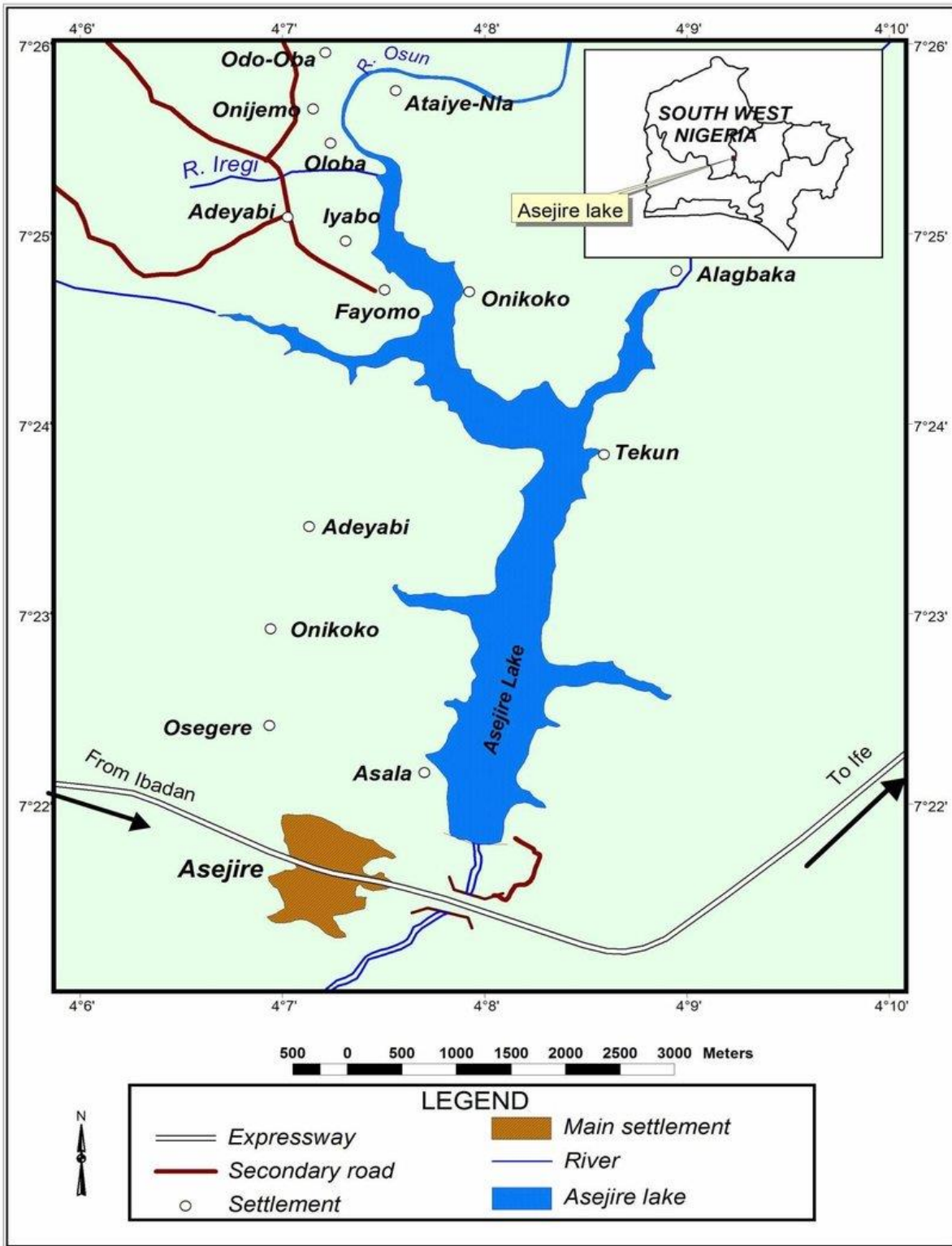


Fig. 1: Location map showing Asejire dam (Ajani *et al.*, 2014)

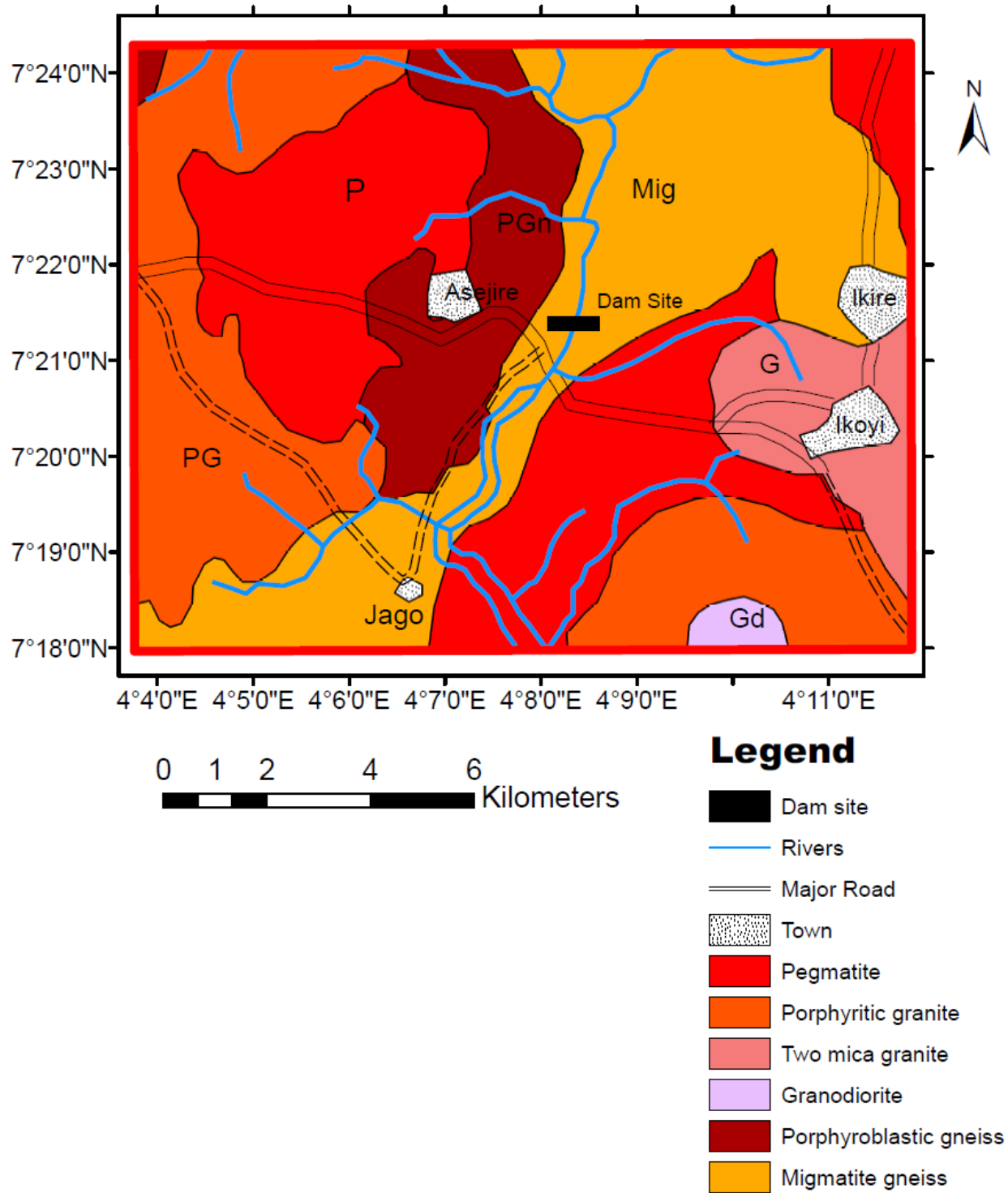


Fig. 2. Geological map showing the study area (modified after Nigerian Geological Survey Agency (NGSA, 2020))

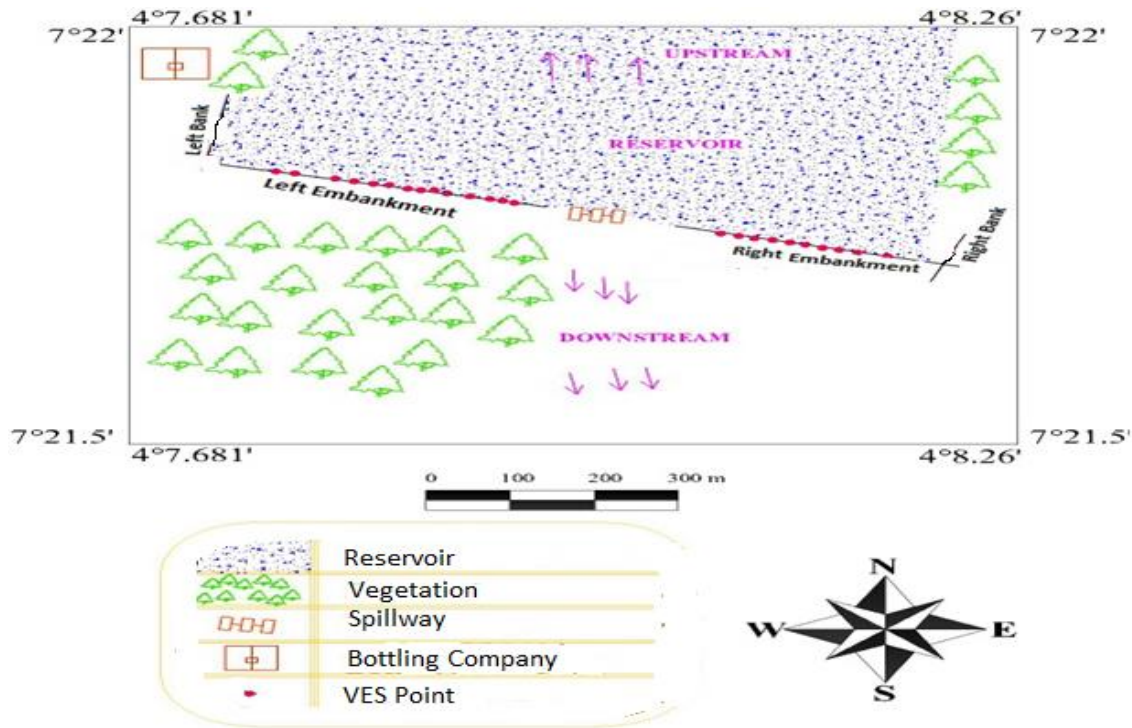


Fig. 3. Field Layout at the study area

electromagnetic fields to produce the characteristic VLF-EM sections beneath the traverses, in which zones of differing conductivity values were delineated (Karous and Hjelt, 1983).

### Vertical Electrical Sounding

The geoelectrical surveys involved Schlumberger vertical electrical sounding (VES) and 2D resistivity profiling. The data were acquired with the aid a resistivity meter and its accessories.

24 sounding stations were occupied along the dam axis with station spacing of 20 m and current electrode spacing (AB/2) varied from 1 m to 100 m. The VES data were interpreted by using partial curve matching technique in which the field curves were superimposed on two-layer master curves and their corresponding auxiliary curves (Orellana and Mooney, 1966) to obtain the starting model parameters which were input for 1D inversion iterative algorithm (Zohdy, 1989). The RMS errors were less than 5%. The layer parameters obtained were used to construct the geoelectric sections on the different geoelectric layers interpreted beneath the sounding points were correlated by using appropriate resistivity ranges inferring lithologies.

## **2D Resistivity Profiling**

The 2D resistivity profiling was carried out along the traverses using dipole-dipole electrode array with electrode spacing,  $a=20$  m and expansion factor,  $n$  varied from 1 to 5. The dipole-dipole data were interpreted using 2D resistivity inversion procedure which iteratively computes the resistivity response of a two-dimensional model until a reasonable match is achieved between a theoretical pseudosection and the observed pseudosection, based on the finite element method (FEM) of modeling using a 2nd order smoothness constraint (Hohnmann, 1982; Loke, 2010).

Integration of different methods is desirable in geophysical investigation so that the results of one method may resolve the ambiguity arising from those of the other(s) and hence enhance the quality of the interpretation (Sharma *et al.*, 2014, Golebiowski *et al.*, 2021).

## **RESULTS AND DISCUSSION**

### **Inverted VLF-EM Sections**

The results of interpretation of the VLF-EM data show two prominently conductive zones suggesting anomalous seepage within the left embankment, lying at horizontal distances of about 280 m and 290 m – 325 m, and depths of about 30 m and 40 m - 55 m respectively (Fig. 4). The relatively less conductive zones observed at other locations within the embankment possibly indicate reduced seepage. They extend from the surface in a somewhat linear and dipping form to about 15 m depth at horizontal distance of about 50 m, about 45 m depth at distance 90 m – 130 m, and about 57 m – 66 m depth between distance 180 m -320 m.

Conductivity is relatively high within the right embankment (Fig. 5). Two prominently conductive zones indicating anomalous seepage occurs beneath horizontal distances of about 250 m and 260 m at depths of about 20 m and 0 m-5 m respectively. The relatively less conductive zones at horizontal distances of 45-50 m (to about 10 m depth), 50- 80 m (to about 15 m depth), 110-150 m (at depth  $\geq 35$  m), and 135-150 m (at 15-25 m depth) possibly suggest reduced seepage. The lower background conductivity beneath the right embankment reflects the fact that it is rock-fill compared to the left embankment which is earth-fill.

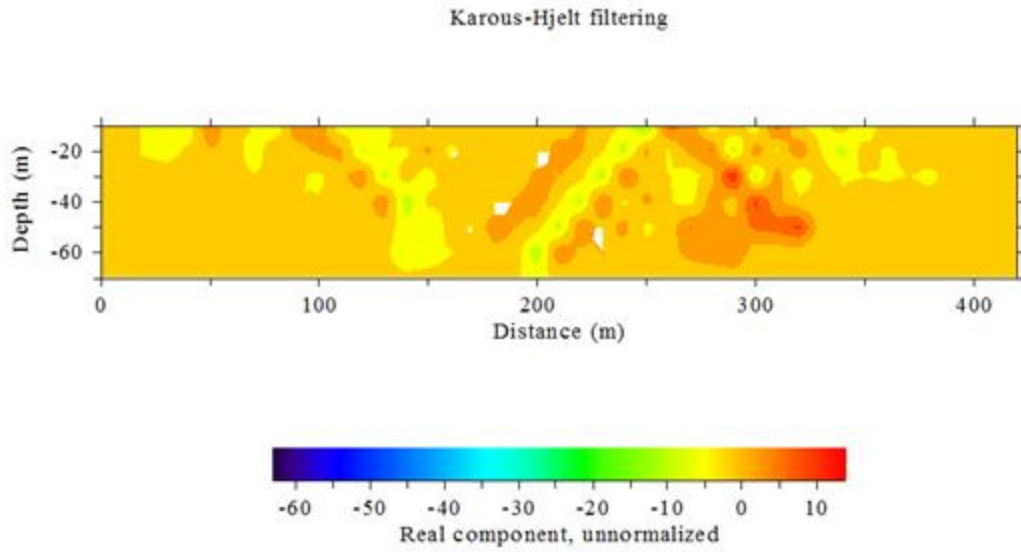


Fig. 4: Inverted VLF-EM section beneath the Left Embankment

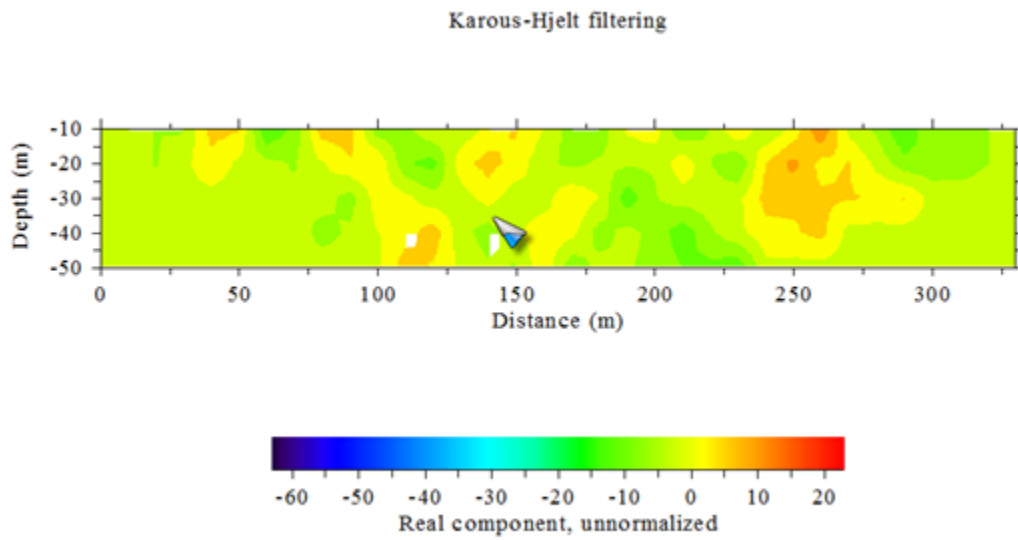


Fig. 5: Inverted VLF-EM section beneath the Right Embankment

## Geoelectric Sections

The characteristic depth sounding curves obtained from the survey are the H-type (Fig. 6). The layer parameters obtained from the interpretation of the VES data are presented in Table 1. The geoelectric section beneath the left embankment reveals three geoelectric layers comprising the caprock, core and the bedrock (Fig. 7). The caprock is has resistivity values ranging from 59  $\Omega$  m to 252  $\Omega$  m, suggesting a clay-sandy clay mix. The layer is 0.7 m-5.2 m thick. The resistivity the core ranges from 23  $\Omega$  m to 64  $\Omega$  m and is characteristic of clay. Its thickness varies from 2.9 m- 37.6 m and is underlain by a more resistive layer which is presumably the basement rock whose resistivity ranges from 121  $\Omega$  m to 1033  $\Omega$  m.

The geoelectric section beneath the right embankment also reveals three geologic layer beneath the rock-fill embankment (Fig. 8). The resistivity of the caprock ranges from 288  $\Omega$  m to 766  $\Omega$  m and its thickness is 0.7 m - 2.2 m. The core has resistivity ranging from 48  $\Omega$  m to 162  $\Omega$  m and thickness varying from 3.1 m to 36.7m. The resistivity of the basement rock varies from 334  $\Omega$  m to 3672  $\Omega$  m. The resistivity vales are higher in this rock-fill right embankment compared to the earth-fill left embankment.

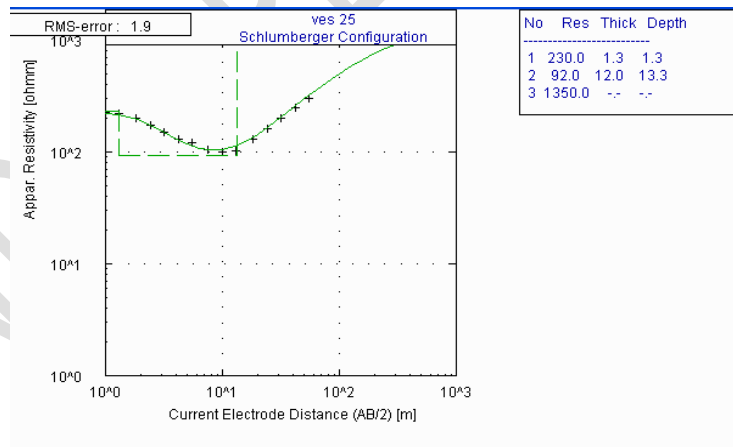


Fig. 6. Typical VES curve obtained in the study area

**TABLE 1: Summary of VES Interpretation**

VES No.	No. of Layers	Resistivity ( $\Omega$ m) $\rho_1/\rho_2/\rho_3$	Thickness (m) $t_1/t_2/t_3$	Depth (m) $h_1/h_2$	Curve type
1	3	82/23/157	0.9/13.3/ $\infty$	0.9/14.2	H
2	3	252/63/96/208	0.7/10.0/ $\infty$	0.7/10.7	H
3	3	118/51/121	1.0/2.9/ $\infty$	1.0/3.9	H
4	3	77/39/910	1.9/25.7/ $\infty$	1.9/37.6	H
5	3	78/34/405	2.3/17.7/ $\infty$	2.3/20.0	H
6	3	93/29/405	1.8/27.1/ $\infty$	1.8/28.9	H
7	3	62/23/320	3.8/33.5/ $\infty$	3.8/37.3	H
8	3	59/44/1816	1.0/35.3/ $\infty$	1.0/36.3	H
9	3	109/43/322	1.0/14.3/ $\infty$	1.0/15.3	H
10	3	77/26/529	5.2/14.3/ $\infty$	5.2/19.5	H
11	3	72/33/499	3.3/27.6/ $\infty$	3.3/30.9	H
12	3	75/31/341	1.8/37.6/ $\infty$	1.8/39.4	H
13	3	129/50/469	1.0/26.9/ $\infty$	1.0/27.9	H
14	3	116/44/949	1.1/37.4/ $\infty$	1.1/38.4	H
15	3	186/55/1033	1.0/28.3/ $\infty$	1.0/29.3	H
16	3	286/73/245	2.2/11.1/ $\infty$	2.2/11.1	H
17	3	303/57/361	1.0/11.3/ $\infty$	1.0/11.3	H
18	3	499/48/857	1.0/12.1/ $\infty$	1.0/13.1	H
19	3	378/77/1407	1.0/3.3/ $\infty$	1.0/4.3	H
20	3	480/110/1608	0.7/8.9/ $\infty$	0.7/9.6	H
21	3	746/109/2027	1.0/36.7/ $\infty$	1.0/37.7	H
22	3	766/113/2209	1.2/36.7/ $\infty$	1.2/37.9	H
23	3	522/103/1764	1.1/3.1/ $\infty$	1.1/4.2	H
24	3	550/162/13672	1.1/12.8/ $\infty$	1.1/13.9	H

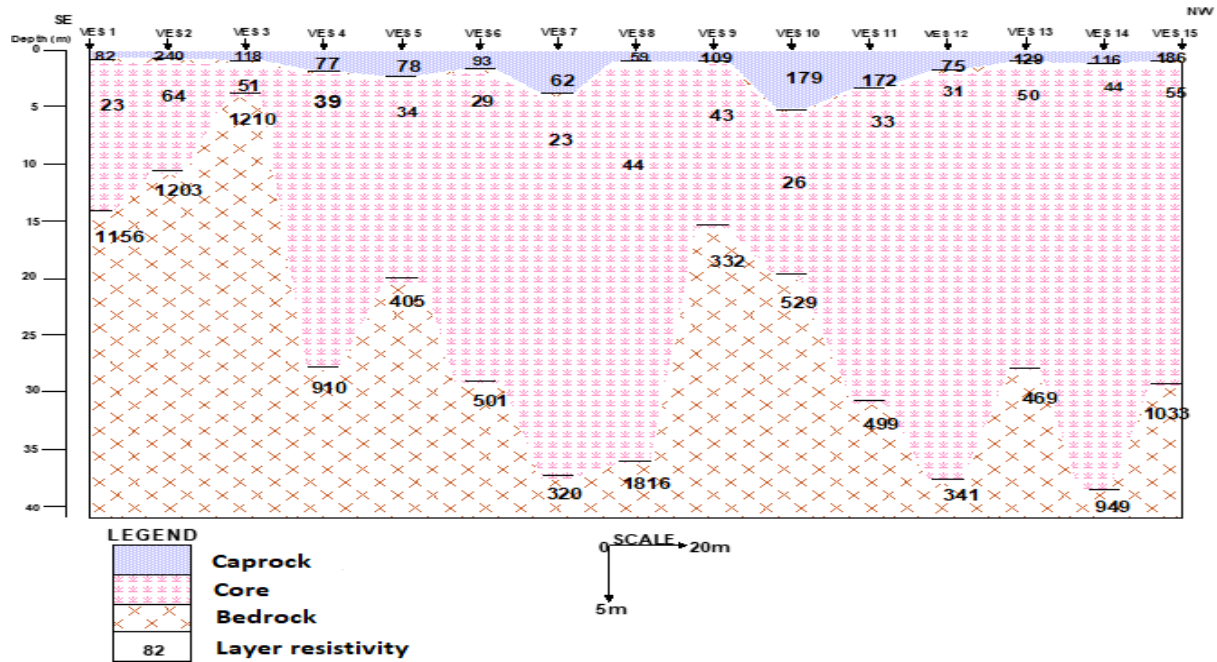


Fig. 7: Goelectric section beneath the Left Embankment

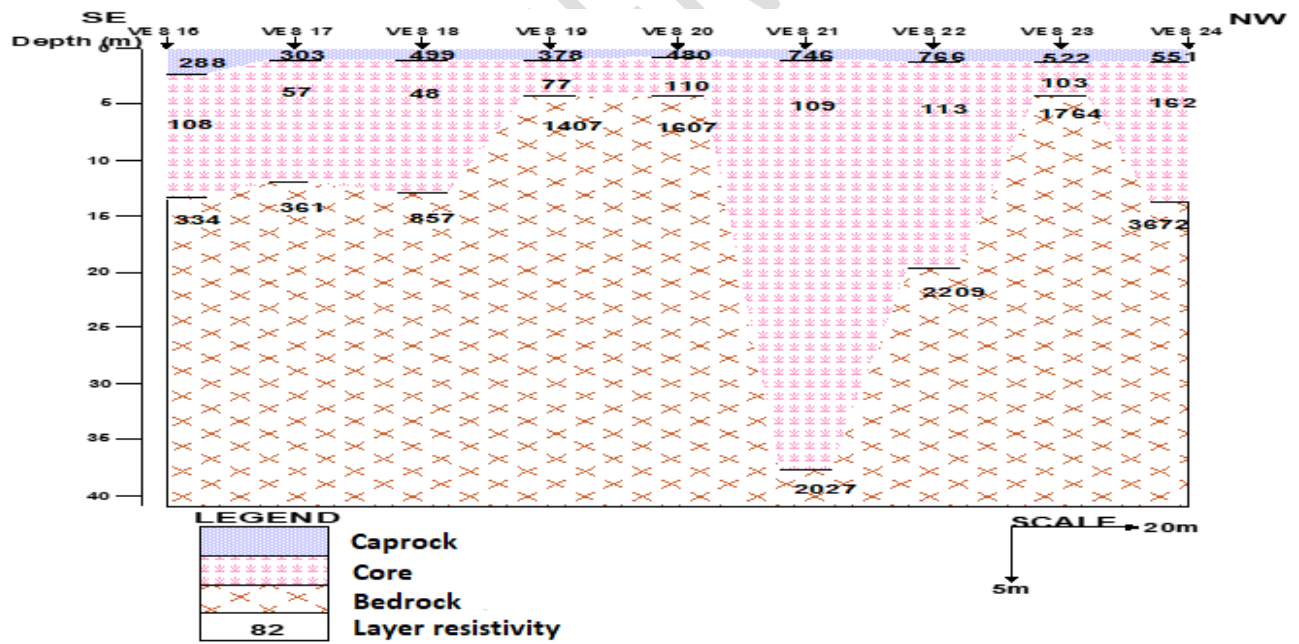


Fig. 8: Goelectric section beneath the Right Embankment

## 2D Resistivity Sections

The 2D inverted resistivity section beneath the left embankment (Fig. 9) reveals a top layer of clay-sandy clay mix of resistivity ranging from 16.8  $\Omega\text{m}$  to 242  $\Omega\text{m}$  underlain by a more resistive basement rock of resistivity varying from 426  $\Omega\text{m}$  to 13201  $\Omega\text{m}$ . The resistivity values less than 1000  $\Omega\text{m}$  indicate weathering. Pockets of anomalously low resistivity values less than 2  $\Omega\text{m}$  observed at 10 m - 20 m depth beneath stations 10-14 are suspected anomalous seepage. The 2D inverted resistivity section beneath the right embankment reveals a top layer with resistivity ranging from 21.1  $\Omega\text{m}$  to 255  $\Omega\text{m}$  underlain by resistive basement with resistivity varying from 311  $\Omega\text{m}$  to 183319  $\Omega\text{m}$  (Fig. 10). Four zones of anomalous resistivity low suggesting anomalous seepage were observed beneath the right embankment beneath stations 2–3 from surface to about 8 m depth, stations 6 - 8, and 9 - 10 at depth from about 8 m to 20 m, and stations 12-15 at depth from 10 m to 30 m.

**LEFT EMBANKMENT (2-D Resistivity Structure)**

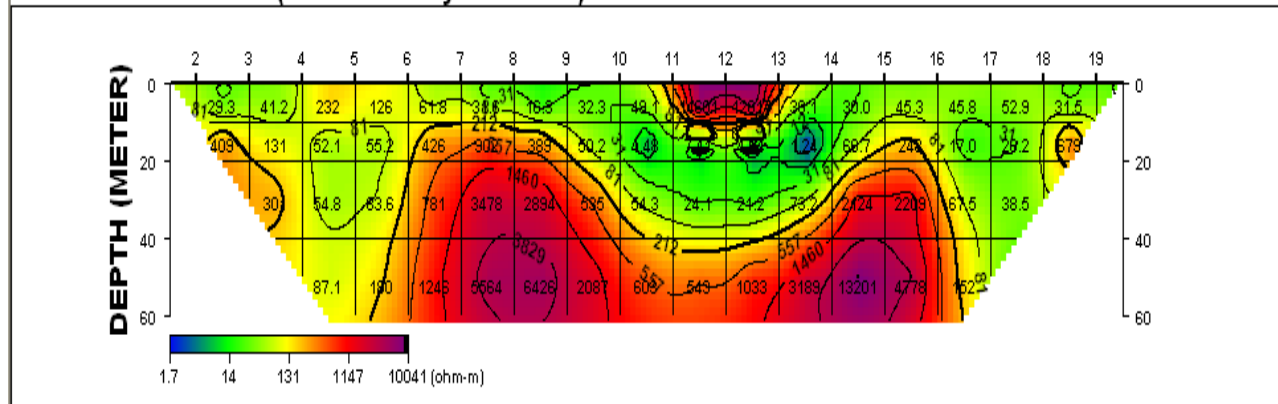


Fig. 9. 2D inverted resistivity section beneath the Left Embankment



## REFERENCES

- Adamo, N., Al-Ansari, N., Sissakian, V., Laue, J., and Knutsson, S., 2020. Geophysical Methods and their Applications in Dam Safety Monitoring Journal of Earth Sciences and Geotechnical Engineering, Vol.11, No.1, 291-345.
- Ademila, O., 2022. Geophysical and Geostatistical Reserve Estimates of Migmatite-Gneiss deposits from parts of Southwestern Nigeria. Global Journal of Geological Sciences vol. 20, 111-130.
- Ahmed, B., Zoe, L. and El-Dakhakhni, W., 2023. Dam system and Reservoir Operational Safety: A Meta-Research. Water, 15 (19), 3427.
- Ajani, E. K., Kareem, O. K., Osho, E. F. and Ekundayo, O. O., 2014. Length-Weight relationship and Condition Factor of *Macrobranchium vollenhovenii* in Asejire Lake. Nigerian Journal of Ecology, Vol. 13, p. 97-111.
- Ajigo, I. O., Odeyemi, I. B. Ademeso, O. A., 2019. Field Geology and Structures of Migmatitic Gneisses Around Ibillo-Okene Area, Southwest Nigeria Journal of Environment and Earth Science, Vol.9, No.2, 59-72.
- Akinlabi I. A. and Ayanrinde O. S., 2018. Geophysical Investigation for anomalous seepage in and around an earth dam embankment in Ogbomoso, southwestern Nigeria. International Journal of Scientific and Engineering Research, vol. 9(7), p. 1455-1467.
- Akinola, O. O. and Obasi, R. A., 2020. Migmatite and Gneisses in the Basement Complex of Southwestern Nigeria: a re-appraisal of their structural, mineralogical, and geochemical diversity, IJRDO – Journal of Applied Sciences, 6 (8), p. 1-17.
- Balogun, O. B., 2019. Tectonic and structural analysis of the Migmatite–Gneiss–Quartzite complex of Ilorin area from aeromagnetic data. NRIAG Journal of Astronomy and Geophysics, Vol. 8, No. 1, p. 22–33.
- Boneli, S. Erosion in geomechanics applied to dams and levees London: Wiley, 2013. 416p.
- Camarero, P. L. and Moreira, C. A., 2017. Geophysical Investigation of Earth dam using the Electrical Tomography Resistivity Technique. Int. Eng. J. Ouro Preto, 70 (1), p. 47-52.
- Fraser, D.C., 1989. Contouring of VLF-EM Data. Geophysics, 54, 245-253.

- Gołębiowski, T.; Piwakowski, B.; Ćwiklik, M.; Bojarski, A. 2021. Application of Combined Geophysical Methods for the Examination of a Water Dam Subsoil. *Water*, 13,2981.
- Hohnmann, G.W., 1982. Numerical modeling for electrical geophysical methods. Proc. Int. Symp. Appl. Geophys. Trop. Reg. Univ. d. Para. Belem. Brazil. p. 308-384.
- Hung, Y., Chou, H. and Lin, C., 2020. Appraisal of the Spatial Resolution of 2D Electrical Resistivity Tomography for Geotechnical Investigation. *Applied Sciences*, 10 (12), 4394-4422.
- Karous, M.R. and Hjelt, S.E. (1983) Linear Filtering of VLF Dip—Angle Measurements. *Geophysical Prospecting*, 31, 782-894.
- Loke, M.H. 2010. *Rapid 2D Resistivity & IP Inversion Using Least-Squares Method*; Tutorial Geotomo Software: Penang, Malaysia.
- Lyu, Z., Cai, J., Xu, Z., Qin, Y. and Cao, J., 2019. A Comprehensive Review on Reasons for Tailings Dam Failures Based on Case History. *Advances in Civil Engineering*, 9, p. 1-18.
- Magawata, U., Mohammed, I., Ojulari, B., Augie, A. and Musa, S., 2020. Geo-Electric Assessment of Kali Failed Dam Project Aliero, North Western Nigeria. *International Journal of Geosciences*, 11 (1), 1-13.
- Magawata, U., Bonde, D., Abdullahi, B., Qudus, B. and Yahaya, M., 2020b. Seepage Investigation on an Existing Dam Using Very Low Frequency Electromagnetic (VLF-EM) Methods: A Case Study of Shagari Earth Dam, Sokoto, North Western Nigeria. *International Journal of Geosciences*, 11 (2), 25-36.
- NGSA, 2020. Geological Maps of Nigeria (Online). A publication of Nigerian Geological Survey Agency, Abuja, Nigeria. Available at: <http://ngsa.gov.ng/geological-maps>.
- Okpoli, C and Tijani, R., 2016. Electromagnetic profiling of Owena Dam, Southwestern Nigeria, using Very-Low-Frequency Radio Fields. *RMZ-M&G*, Vol. 63, p. 237-250.
- Oladimeji, T. E. and Olaosebikan, T. O., 2017. Morphological Variability of *Tilapia Zillii* (Gervais, 1848) from selected Reservoirs in Southwestern, Nigeria. *Ife Journal of Science*, Vol. 19, no. 1, p. 15 -25.
- Olasunkanmi, N. K., Aina, A., Olatunji, S., Bawalla, M., 2018. Seepage Investigation on an Existing Dam using Integrated Geophysical Methods. *Journal of Environment and Earth Science*, Vol.8, No.5, p. 6-16.

Olasunkanmi, N. K., Sunmonu, L. A., Owolabi, D. T., Bawallah, M., Oyelami, A., 2021. Investigation of Dam Integrity from Electrical Resistivity Methods: A case of Erelu Dam, Southwestern Nigeria. *Indonesian Journal of Geoscience* 8 (2), p. 265-274.

Orellana, E and Mooney, H.M., 1972. *Mater curves for Vertical Electrical Soundings over layered structures*, Interciencia, Madrid.

Pawley, M. J., Reid, A. J., Dutch, R. A. and Preiss, W. V., 2015. Demystifying migmatites: An Introduction for the Field-Based Geologist; *Applied Earth Science (Transactions of the Institutions of Mining and Metallurgy, Section B)*, 124(3): 147-174.

Rahaman, M.A., 1989. Review of the geology of southwestern Nigeria. In: *Geology of Nigeria, 2<sup>nd</sup> Edition.*, (Kogbe C.A., Ed.) – Rock View (Nig.) Ltd., Jos, p. 39-56.

Sharma, S., Biswas, A., and Baranwal, V., 2014. Very Low-Frequency Electromagnetic Method: A Shallow Subsurface Investigation Technique for Geophysical Applications, *in* Sengupta, D., ed., *Recent Trends in Modelling of Environmental Contaminants: New Dehli*, Springer India, p. 119-141.

Sungkono, S, Husein, A, Prasetyo, H, Bahri, A. S., Monteiro Santos, F. A., Santosa, B. J., 2014. The VLF-EM imaging of potential collapse on the LUSI embankment. *Journal of Applied Geophysics*, Vol. 109, p. 218-232.

Utete, B. and Fregene, B. T., 2020. Assessing the spatial and temporal variability and related environmental risks of toxic metals in Lake Asejire, south-western Nigeria, p. 1-15.

Zohdy, A. A. R., 1989. A new method for the automatic interpretation of Schlumberger and Wenner sounding curves. *Geophysics*, 54, 245-253.